Electronic Supplementary Information

Acid-triggered *in vivo* aggregation of Janus nanoparticles for enhanced imaging-guided photothermal therapy

Ruixue Wei,[*a] Zhe Li,[a] Bilun Kang,[b] Gaoliang Fu,[c] Ke Zhang,[*d] and Mengzhou Xue[*a]

[a]Department of Cerebrovascular Diseases, The Second Affiliated Hospital of Zhengzhou University, Zhengzhou 450052, Henan, China.

[b]State Key Laboratory of Physical Chemistry of Solid Surfaces, The MOE Laboratory of Spectrochemical Analysis & Instrumentation, and The Key Laboratory for Chemical Biology of Fujian Province, College of Chemistry and Chemical Engineering, Xiamen University, Xiamen 361005, Fujian, China.

[c]Henan Provincial Key Laboratory of Nanocomposites and Applications, Institute of Nanostructured Functional Materials, Huanghe Science and Technology College, Zhengzhou 450006, Henan, China.

[d]Department of Interventional Medicine, Center for Interventional Medicine, Guangdong Provincial Engineering Research Center of Molecular Imaging, and Guangdong Provincial Key Laboratory of Biomedical Imaging, The Fifth Affiliated Hospital, Sun Yat-sen University, Zhuhai 519000, Guangdong, China.

*Email: wei2009ruixue@163.com

*Email: zhangk276@mail.sysu.edu.cn

*Email: xuemengzhou@zzu.edu.cn

Experimental Section

Materials

All the chemical reagents were used as received without further purification. 1-octadecene (1-ODE, tech, 90%) were purchased from Acros Organic. Oleic acid (OA, tech, 90%) and oleylamine (OAm, tech, 90%) were purchased from Alfa Aesar. Dopamine hydrochloride, 3, 4-dihydroxyhydrocinnamic acid (DHCA) 1, 2-hexadecanediol, iron acetylacetonate ($Fe(acac)_3$), and gold acetate were purchased from Sigma-Aldrich. Other reagents were purchased from Sinopharm Chemical Reagent.

Characterization

Transmission electron microscopy (TEM) images and high-resolution transmission electron microscopy (HRTEM) images were captured on a JEOL JEM-2100 microscope with an acceleration voltage of 200 kV. The concentrations of Au and Fe in the samples were measured by inductively coupled plasma atomic emission spectroscopy (ICP-AES). The amounts of Au in the organs and tumor were measured by inductively coupled plasma-mass spectrometry (ICP-MS). X-ray powder diffraction (XRD) patterns were carried out on a Rigaku UltimaIV X-ray diffractometer, and equipped with a Cu Kα radiation source (λ = 0.15418 nm). Field-dependent magnetization (M−H) curves were obtained *via* a superconducting quantum interference device (SQUID). Hydrodynamic diameters of nanomaterials were measured *via* dynamic light scattering (DLS) on a Malvern Zetasizer nano ZS instrument. Cell fluorescent photographs were taken using a fluorescence microscope (OLYMPUS). T_1/T_2 relaxation time and T_1-/T_2-weighted phantom images were carried out on a 20 MHz NMI20-Analyst NMR Analyzing and Imaging system (Suzhou Niumag Analytical Instrument Corporation, Suzhou, China). *In vivo* MRI were performed on a 4.7 T MRI scanner (MR SOLUTIONS). *In vivo* PAI were performed on PAI scanner (Vevo LAZR-X, Fujifilm VisualSonic).

Synthesis of gold-iron oxide Janus nanoparticles (GIJ NPs)

GIJ NPs was synthesized according to previous reports with minor modification.[1] In a typical experiment, 176 mg of ferric acetylacetonate ($Fe(acac)_3$), 53 mg of gold acetate ($Au(Ac)_3$), 0.48 mL of oleic acid (OA), 0.48 mL of oleylamine (OAm), 645 mg of 1, 2-hexadecanediol, and 15 mL of 1-octadecylene (1-ODE) were mixed at room temperature. The resulting solution were degassed under vacuum at 100 ˚C for 30 min, and then were heated to 320 ˚C for 90 min after heated 200 ˚C for 30 min. After cooled to room temperature, the product was precipitated by the mixture of *n*-hexane and ethyl alcohol (1:1 v/v), and washed three times by ethyl alcohol. The products were dispersed in *n*-hexane.

Synthesis of trimethylammonium dopamine (TMAD)

We synthesis trimethylammonium dopamine (TMAD) according to a reported method (Figure S2)[2]. Iodomethane (1.69 mmol) was added to 3 mL of ethyl acetate containing of 0.527 mmol of dopamine hydrochloride and 1.58 mmol of potassium carbonate. The resulting solution was stirred for 72 h at room temperature. The mixture was concentrated and the residue was subjected to semi-recrystallizations using methanol four times. The product residue was dissolved in a minimum amount of methanol at a time and then vacuum filtered to separate out the excess salt. The filtrate was rotovaped to obtain a brown flakey product.

Synthesis of water-dispersible GIJ NPs

3,4-dihydroxyhydrocinnamic acid (DHCA, 25 mg) and trimethylammonium dopamine (TMAD, 10 mg) were dissolved in 5 mL deionized water, and adjusted pH value to 9 by 1 M NaOH solution before 5 mL of acetone was added. *n*-hexane (4 mL) containing about 10 mg of GIJ NPs was added to the above solution. The resulting mixture were stirred for 5 h at 40 ˚C under a nitrogen atmosphere. The DHCA and TMAD co-coated GIJ NPs were collected by centrifugation and re-dispersed in deionized water (denote as GIJ@DHCA-TMAD). The process of DHCA coating GIJ is same as above, but without adding TMAD, the water-dispersible product is noted as GIJ@DHCA.

Relaxivity measurement and MRI phantom studies

T_1 and T_2 relaxation time and T_1-/T_2-wighted phantom images of GIJ@DHCA-TMAD and GIJ@DHCA were acquired on a 0.5 T NMI20-Analyst NMR Analyzing and Imaging system. The samples were dispersed in PBS buffer (pH = 7.4 or 5.5) with different Fe concentrations at 0.4, 0.2, 0.1, 0.05, 0.025 mM. The r_1 and r_2 were calculated from the slopes of the best fitted lines of 1/T versus manganese. The T_1-/T_2-weighted phantom images were acquired with the following parameters: TR/TE = 200/2 ms (T_1), TR/TE = 2000/40 ms (T_2), NS = 2.

Cytotoxicity Assay

The 4T1 cells were purchased from the Cell Bank of the Chinese Academy of Sciences (Shanghai, China). Cytotoxicity was assayed *via* Cell Counting Kit-8 (CCK8) using 4T1 cells (n = 5 /group). The 4T1 cells were seeded into 96-well plate at 4×10^3 cells per well and incubated for 24 h. Then, the cells incubated with GIJ@DHCA-TMAD or GIJ@DHCA for 24 h at different concentrations (0.8, 1.6, 6.4, 2.5, 50, and 100 μg/mL). 10 μL of CCK-8 reagent (C0037, Beyotime Institute of Biotechnology, Haimen, China) was added to each well, followed by 4 h of incubation at 37 °C. Finally, the absorbance was measured at 450 nm on a Multiskan FC microplate reader.

Photothermal conversion effect

GIJ@DHCA-TMAD was dispersed in PBS buffer (pH = 7.4 or 5.5), and was diluted into different concentration gradients with concentrations of 0, 20, 49, 80, and 160 μg Au /mL, respectively. Then 2 mL was placed in a quartz colorimetric dish, and a laser at 808 nm was applied with a laser density of 1 W/cm^2 for 5 min. The portable thermocouple is just immersed below the liquid level (to prevent laser specks from hitting the probe) and a temperature value is read every 20 s.

4T1 cells were divided into 4 groups and cultured in a 3.5 cm cell culture dish with a density of 1×10^5. 4T1 cells were cultured by adding samples (Blank, Laser only, GIJ@DHCA + laser, GIJ@DHCA-TMAD

+ laser) with concentration of 100 μg Au /mL for 4 h, 808 nm laser was applied to the cells for 5 min with a laser density of 1 W cm^2. After that, the medium was removed, washed with PBS three times, and 1 mL medium was added again. At the same time, fluorescent dye Calcein AM and pyridine iodide (PI) were added to the cell culture medium to indicate living cells and dead cells, and mixed for 5 min. The culture medium was removed and washed with PBS for three times. Finally, the cell survival was photographed by fluorescence microscope.

Calculation of the photothermal conversion efficiency (η).

The η was calculated according to the energy balance of the system,[3, 4] which is displayed as follows:

$$\eta = [hS (T_{max} - T_{surr}) - Q_S] / (I - 10^{-A808}I) \qquad \text{Equation S1}$$

h is the heat transfer coefficient; S is the surface area of the container. Q_S is heat dissipated from the laser mediated by the solvent and container. I is the laser power and A_{808} is the absorbance at 808 nm.

$$\tau_S = m_S C_{water} / (hS) \qquad \text{Equation S2}$$

m_S is the mass of the solution containing GIJ@DHCA-TMAD. C_{water} is the specific heat capacity of water (C_{water} = 4.2 J/g/°C). τ_S is the associated time constant.

$$t = -\tau_S \ln(\theta) \qquad \text{Equation S3}$$

θ is a dimensionless parameter, known as the driving force temperature.

$$\theta = (T - T_{surr}) / (T_{max} - T_{surr}) \qquad \text{Equation S4}$$

T_{max} and T_{surr} are the maximum steady state temperature and the environmental temperature, respectively.

The photothermal conversion efficiency of GIJ@DHCA-TMAD was evaluated by using the 808 nm laser for irradiation.

Blood circulation half-life

We injected GIJ@DHCA-TMAD and GIJ@DHCA intravenously into healthy mice at same dose (10 mg Au and 10 mg Fe per kg body weight) to measure the blood circulation half-lives. At different time points

(5 min, 10 min, 30 min, 1 h, 2 h, 4 h, 8 h, 24 h) after administration, 20 μL of blood was taken from the tail vein of mice and digested with 69% HNO_3 and 30% H_2O_2 (v(HNO_3)/v(H_2O_2) = 3:1). The resulting solution was diluted with 2% HNO_3 and filtered through a 0.22 μm filter membrane. The concentrations of Au and Fe in the samples were determined by ICP-MS.

Biodistribution in tumor-bearing mice

Tumors were inoculated by injecting 4T1 cells into subcutaneous tissues according to a reported method.[5] GIJ@DHCA-TMAD and GIJ@DHCA were intravenously injected into 4T1 tumor-bearing mice at dose of 10 mg Au and 10 mg Fe per kg body weight. The mice were sacrificed at 24 h after administration, and the major organs (heart, liver, spleen, lung, kidney, and tumor) were collected and weighted. After digested with 69% HNO_3, the resulting solution were diluted with 2% HNO_3 and filtered through a 0.22 μm filter membrane. The concentrations of Au and Fe in the samples were determined by ICP-MS.

***In vivo* MRI study**

Animal experiments were executed according to the protocol approved by the Institutional Animal Care and Use Committee of Zhengzhou University. MR imaging was performed on a 4.7 T MRI scanner. Male BALB/c mice (18~22 g) were used for *in vivo* MR imaging (n = 3/group). Tumors were inoculated by injecting 4T1 fragments into subcutaneous tissues. When the tumors grew into about 5 mm in diameter, the mice were used to *in vivo* MR imaging. GIJ@DHCA-TMAD or GIJ@DHCA were tail vein intravenously injected into mice (at a dose of Fe = 2 mg per kg body weight). The T_2-weighted MR images were acquired at different times after administration using fsems sequence with the following parameters: TR/TE = 3000/40 ms, thickness = 1.5 mm, data matrix (RO × PE) = 256 × 256. SNR was calculated by the following equation:

$$SNR = SI_{tumor} / SD_{noises}$$

***In vivo* PAI study**

Animal experiments were executed according to the protocol approved by the Institutional Animal Care and Use Committee of Zhengzhou University. MR imaging was performed on a 4.7 T MRI scanner. Male BALB/c mice (18~22 g) were used for *in vivo* MR imaging (n = 3/group). Tumors were inoculated by injecting 4T1 fragments into subcutaneous tissues. When the tumors grew into about 5 mm in diameter, the mice were used to *in vivo* MR imaging. GIJ@DHCA-TMAD or GIJ@DHCA were tail vein intravenously injected into mice at a dose of 2 mg Au per kg.

***In vivo* Therapeutic Study**

Animal experiments were executed according to the protocol approved by the Institutional Animal Care and Use Committee of Zhengzhou University. Male BALB/c nude mice (18~22 g) bearing subcutaneous murine sarcoma 4T1 were used for *in vivo* therapeutic study. The mice were randomly divided into 4 groups (n = 5/group): GIJ@DHCA-TMAD + laser, GIJ@DHCA + laser, laser only, and PBS. When the tumors reached approximately 5 mm in diameter, the mice were tail vein intravenously injected with GIJ@DHCA-TMAD at a dose of 2 mg Au per kg body weight. The control groups were injected with the same volume of GIJ@DHCA or PBS. After 1 h, 808 nm laser was applied to the tumor for 5 min with a laser density of 1 W/cm^2. At the same time, we used infrared thermal imager to record the temperature change of laser irradiation for 5 min, and recorded the temperature every 30 s to draw the temperature curve. The tumor volumes and the mice weights were monitored every three days for three weeks. The tumor volume was calculated according to the following equation:

$$V_{tumor} = (d_{max}^2 \times d_{min}) / 2$$

Histological Examination

After various treatment of 30 days, the mice were sacrificed. The major organs and tumors were collected, weighted, fixed in polychlorinated formaldehyde, embedded in paraffin, sectioned and stained with hematoxylin and eosin. The histological sections were analyzed on microscope.

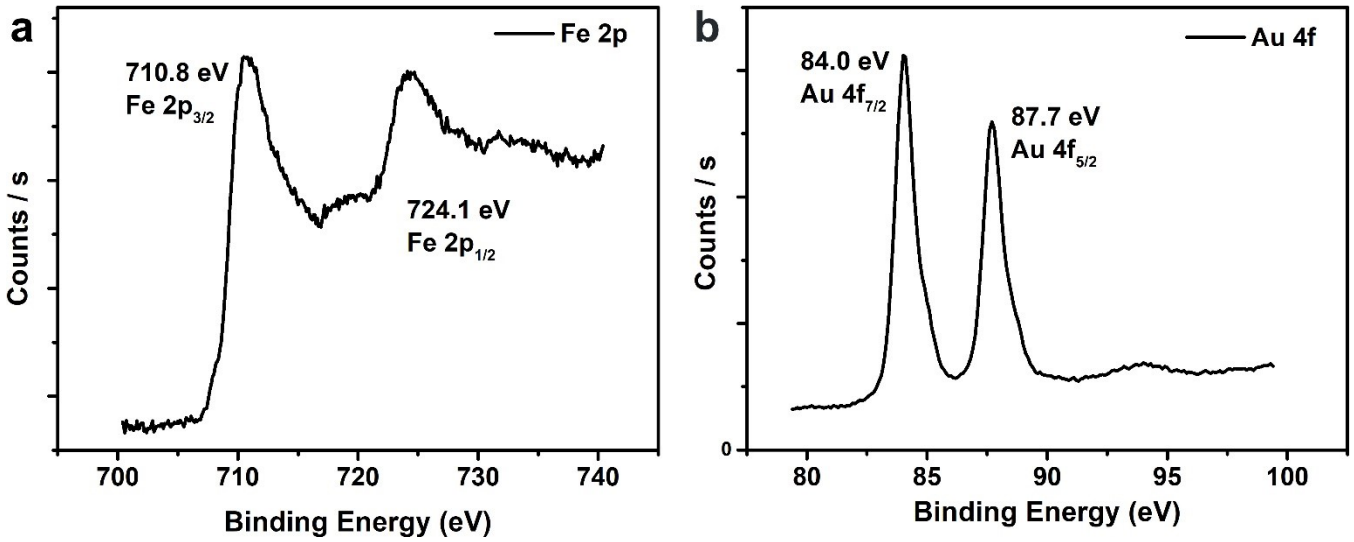

Figure S1. The X-ray photoelectron spectroscopy (XPS) of GIJ NPs. The peaks of (a) Fe $2p_{3/2}$ (710.8 eV), Fe $2p_{1/2}$ (724.1 eV), and (b) Au $4f_{7/2}$ (84.0 eV), Au $4f_{5/2}$ (87.7 eV) indicated the state of Fe and Au, respectively.

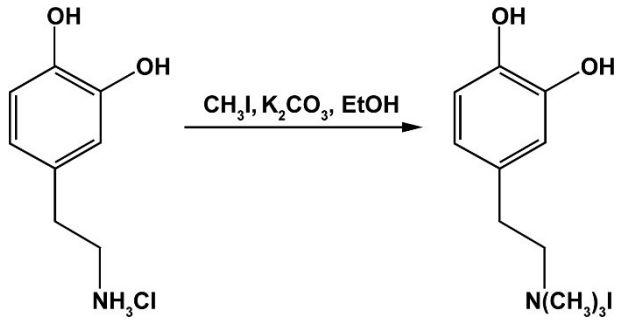

Figure S2. Synthesis of trimethylammonium dopamine (TMAD).

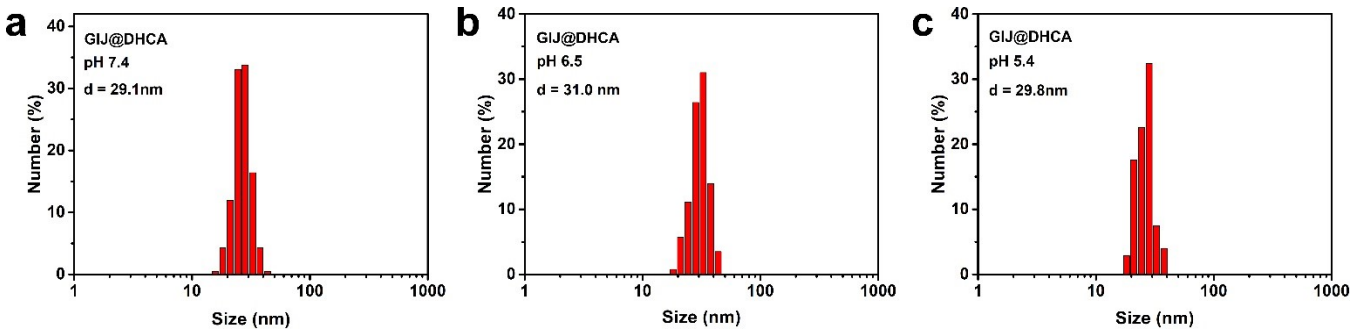

Figure S3. The dynamic light scattering of GIJ@DHCA at pH (a) 7.4, (b) 6.5, and (c) 5.5.

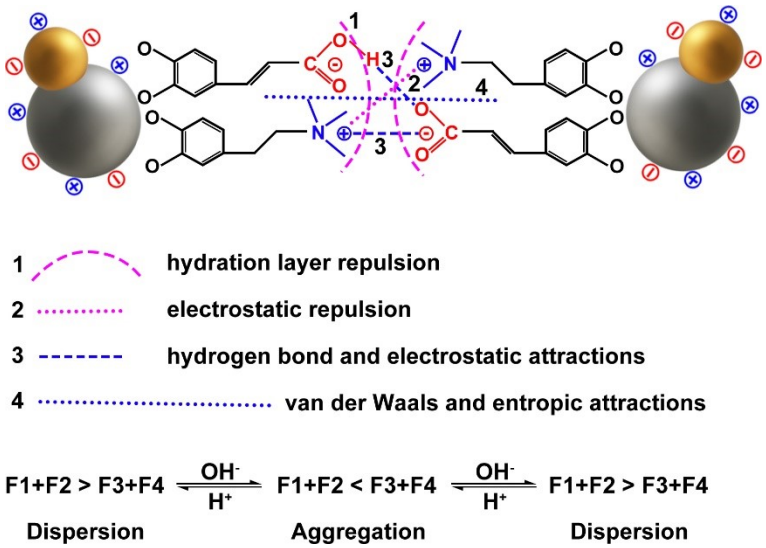

Figure S4. A possible mechanism for the pH-responsive aggregation of GIJ@DHCA-TMAD. At high pH, GIJ@DHCA-TMAD were stabilized in solution by strong hydration and electrostatic repulsions. The strong hydration layer on the mixed charged nanoparticles surface makes them be quite stable in solution with high ionic strength, where the electrostatic repulsions are screened.[6] When the pH decreased to certain value, partial protonation of DHCA ligands leads to attraction of hydrogen bonds, and nanoparticles aggregated when the overall attractions of the van der Waals force and hydrogen bonding surpassed the hydration and electrostatic repulsions. As the pH continue decreased, more DHCA ligands were protonated, the electrostatic repulsions of positive quaternary ammonium surpassed the attractions of the van der Waals force and hydrogen bonding, GIJ@DHCA-TMAD become dispersion again.

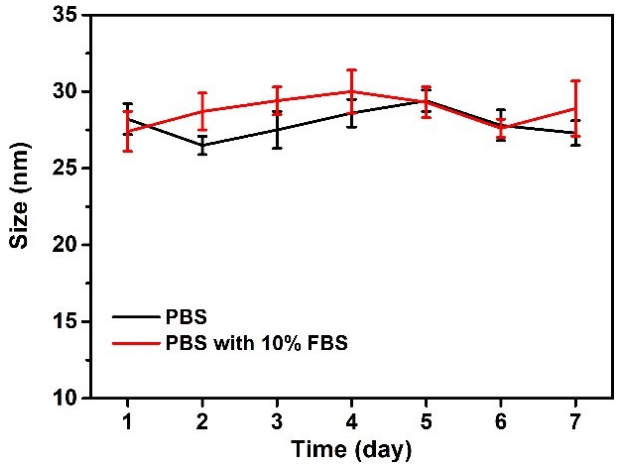

Figure S5. The hydrodynamic diameter of GIJ@DHCA-TMAD in phosphate buffer (1× PBS, pH = 7.4) and 10% (v/v) fetal bovine serum (FBS) solution.

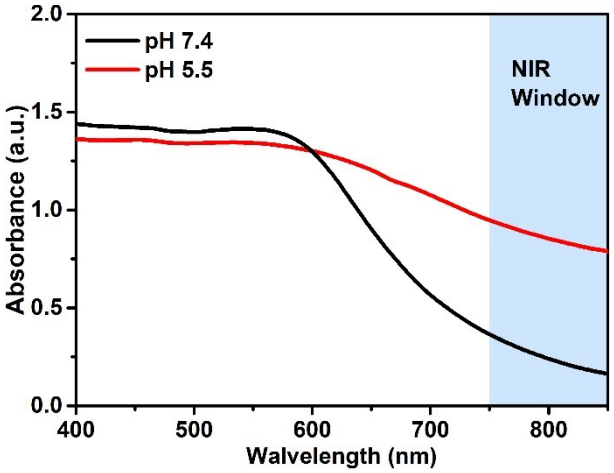

Figure S6. UV−vis spectrum of GIJ@@DHCA-TMAD at pH 7.4 and 5.5 in PBS solution.

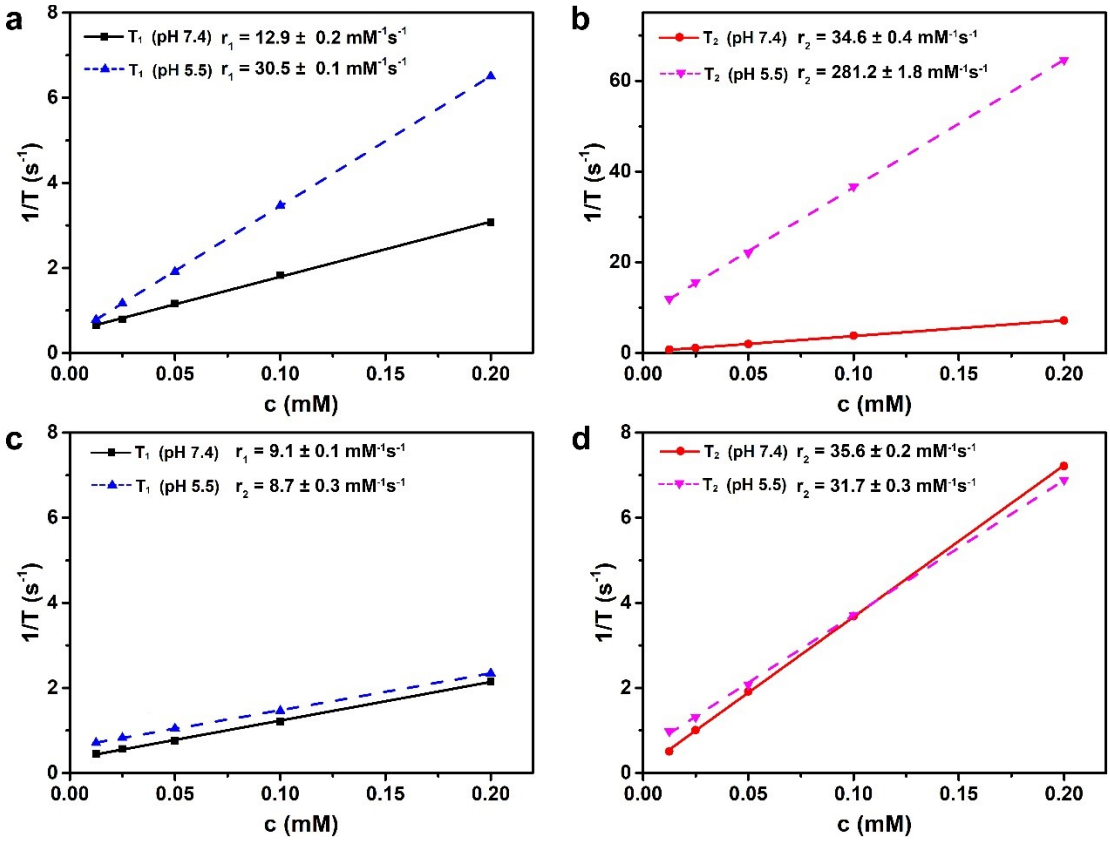

Figure S7. Relaxivity measurements of GIJ NPs. (a) r_1 and (b) r_2 analysis of GIJ@DHCA-TMAD at different pH values (7.4 and 5.5). (c) r_1 and (d) r_2 analysis of GIJ@DHCA at different pH values (7.4 and 5.5). The r_1 and r_2 values were calculated from the slopes of best linear fits.

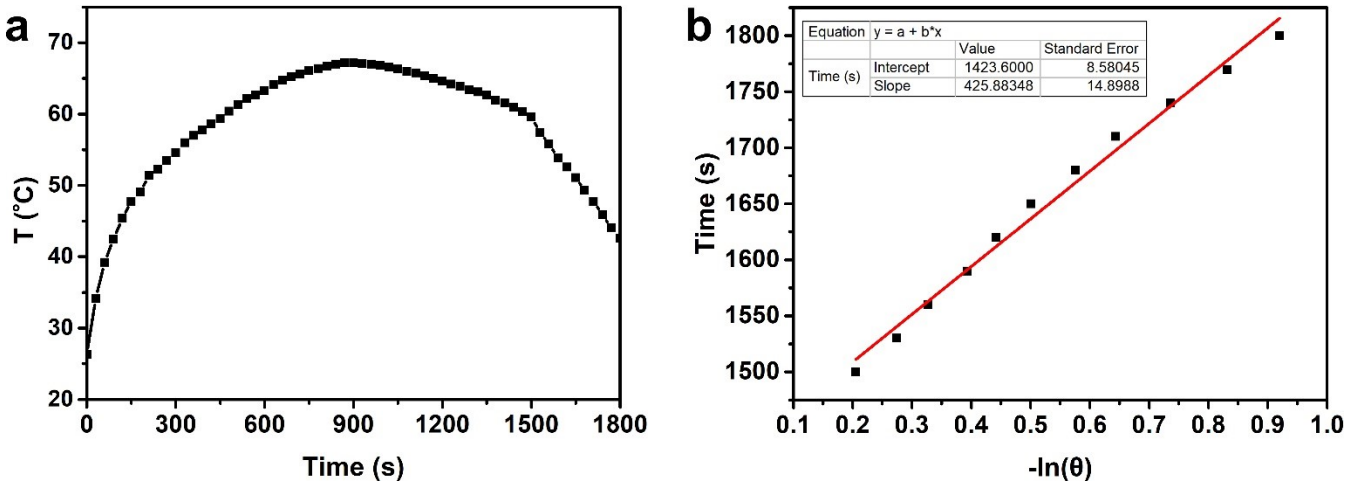

Figure S8. (a) Photothermal effect of the GIJ@DHCA-TMAD aqueous solution under laser irradiation (808 nm, 1 W/cm^2, 1500 s) at pH 5.5, and then the laser was turned off. (b) The slope of the fitted line from the time point of the cooling period (after 1500 s) with the corresponding -ln(θ) is obtained: τ_S was 425.9 s. θ is the dimensionless parameter.

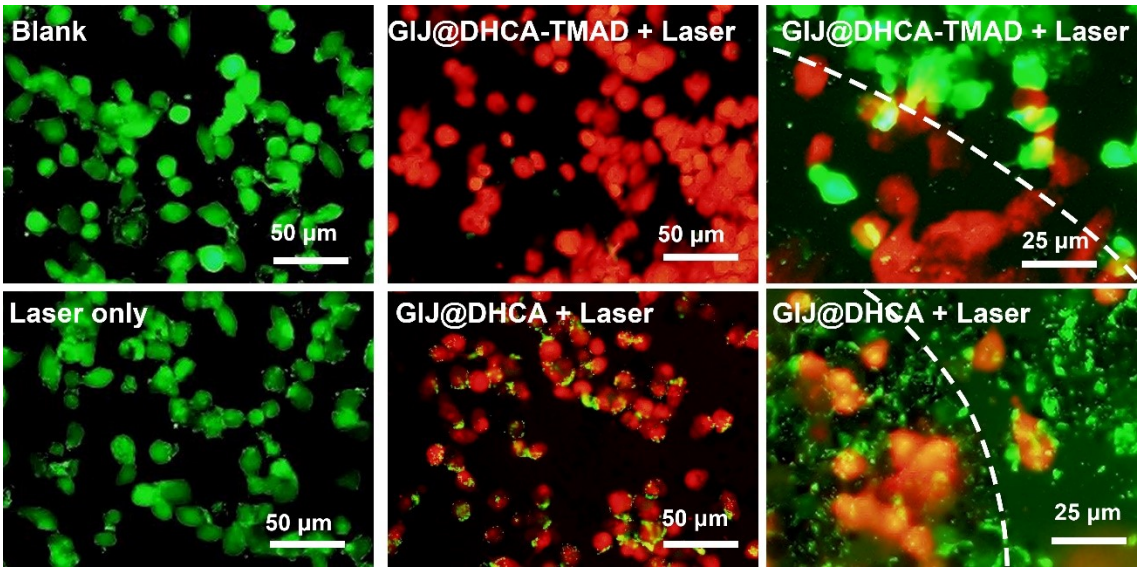

Figure S9. The merged fluorescence images of 4T1 cells stained with Calcein AM /PI kit for showing the thermal ablation effects of GIJ@DHCA-TMAD and GIJ@DHCA with 808 nm laser irradiation (1 W/cm^2, 5 min).

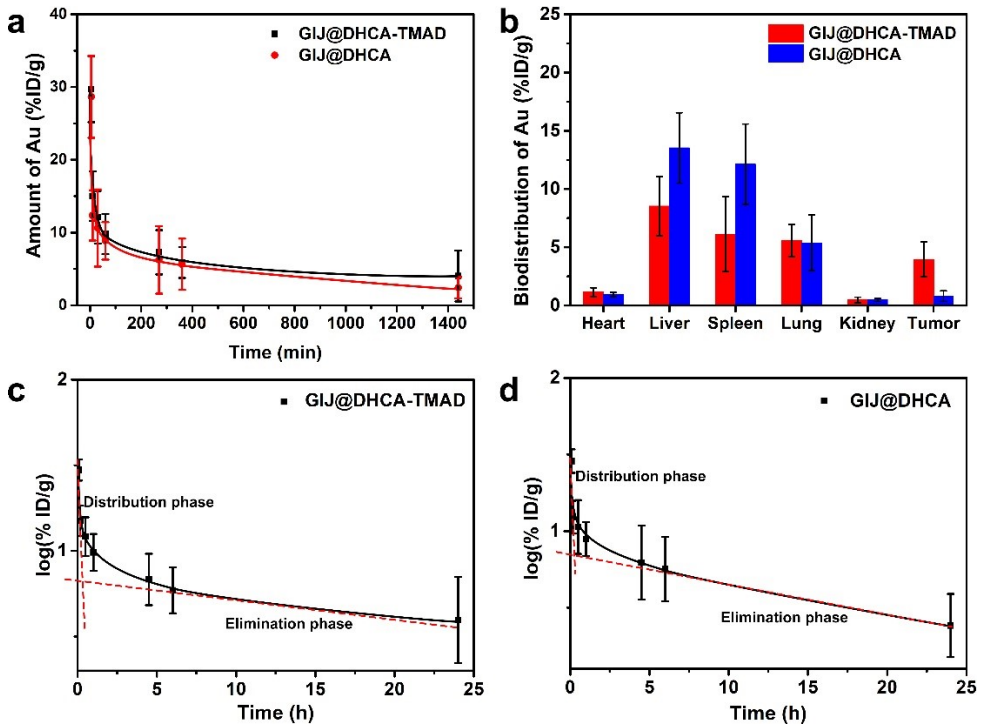

Figure S10. (a) Blood circulation curves of Au after intravenous injection of GIJ@@DHCA-TMAD or GIJ@DHCA. (b) Biodistribution of Au at 24 h after intravenous injection of GIJ@@DHCA-TMAD or GIJ@DHCA at a dose of 10 mg Au per kg body weight (n = 3 per group). The log(%ID/g)-time curves of Au after intravenous injection of (c) GIJ@DHCA-TMAD and (d) GIJ@DHCA. The $t_{1/2\alpha}$ and $t_{1/2\beta}$ of GIJ@DHCA-TMAD were calculated to be 1.2 h and 25.1 h, respectively. The $t_{1/2\alpha}$ and $t_{1/2\beta}$ of GIJ@DHCA were calculated to be 1.1 h and 14.4 h, respectively. α and β are the hybrid constants.

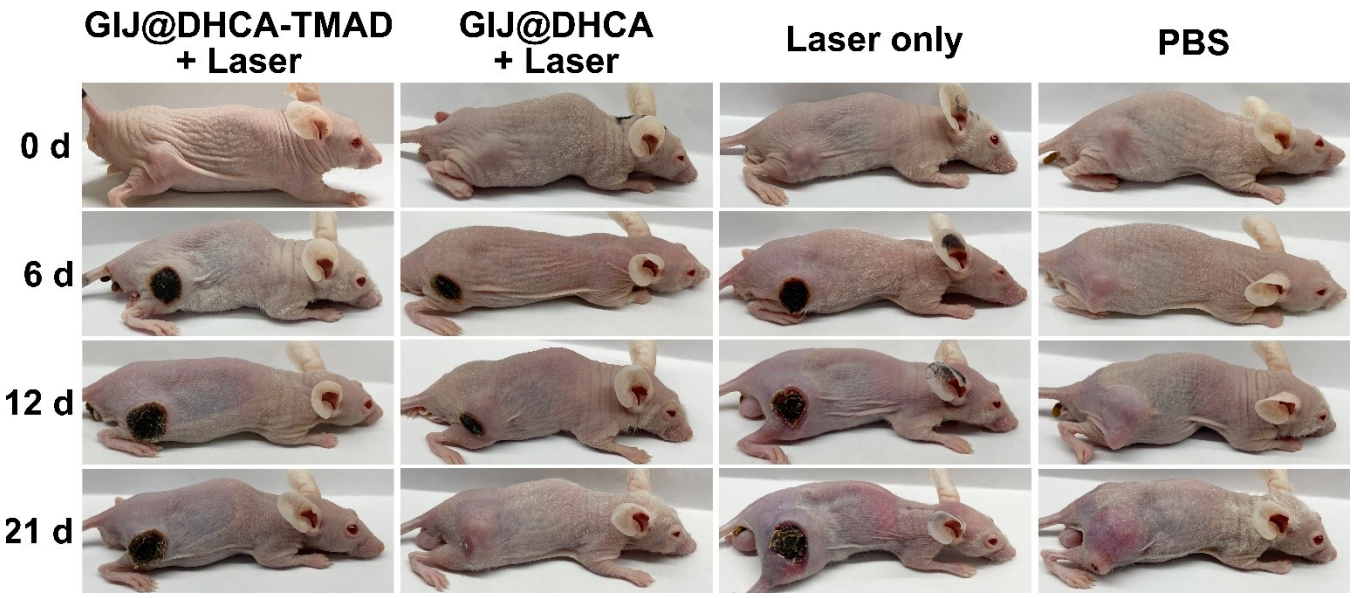

Figure S11. Representative digital photographs of one mouse per group taken at the indicated time points after different treatments. Mice bearing subcutaneous 4T1 tumors.

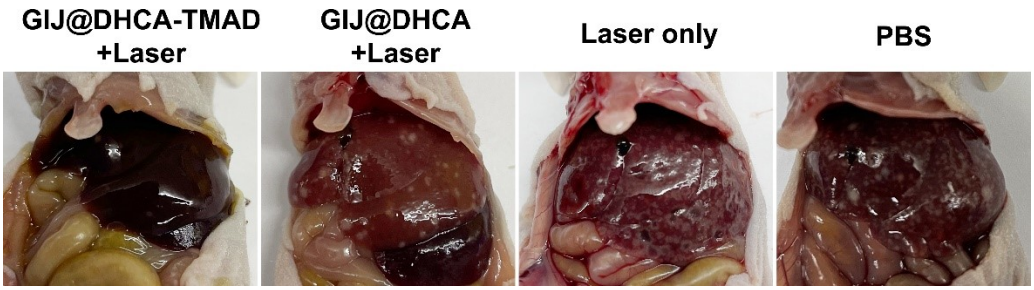

Figure S12. Liver taken from each group after 30 days treatment.

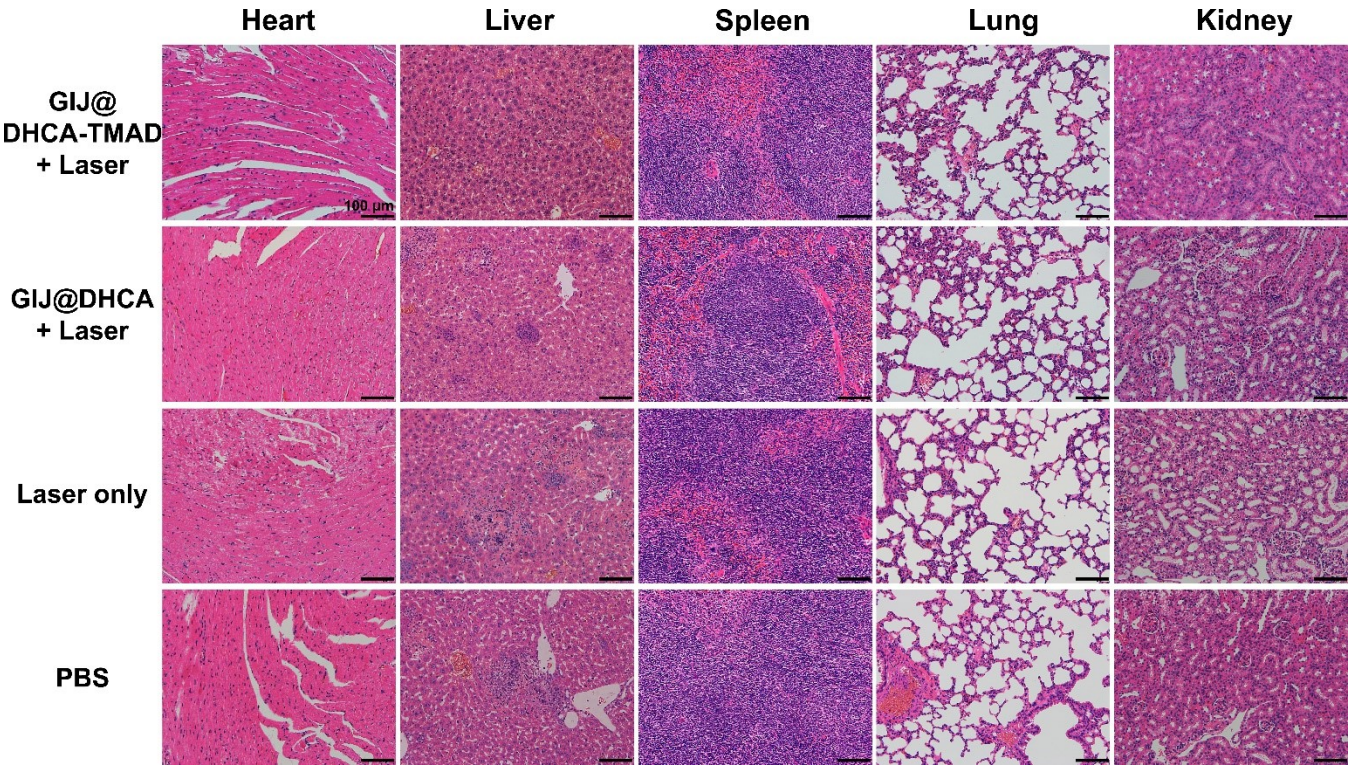

Figure S13. H&E histology images of heart, liver, spleen, lung, and kidney of the mice after treatment with GIJ@@DHCA-TMAD + laser, GIJ@DHCA + laser, laser only or PBS for 30 d.

References

1. J. Gallo, I. García, D. Padro, B. Arnáiz and S. Penadés, *J. Mater. Chem.*, 2010, **20**, 10010-10020.
2. J. L. Collins, 3rd, A. Fujii, S. Roshandel, C.-A. To and M. P. Schramm, *Bioorg. Med. Chem. Lett.*, 2017, **27**, 2953-2956.
3. Z. Zhao, C. Chen, W. Wu, F. Wang, L. Du, X. Zhang, Y. Xiong, X. He, Y. Cai, R. T. K. Kwok, J. W. Y. Lam, X. Gao, P. Sun, D. L. Phillips, D. Ding and B. Z. Tang, *Nat. Commun.*, 2019, **10**, 768.
4. L. Wang, H. Lin, X. Chi, C. Sun, J. Huang, X. Tang, H. Chen, X. Luo, Z. Yin and J. Gao, *Small*, 2018, **14**, 1801612.
5. R. Wei, X. Gong, H. Lin, K. Zhang, A. Li, K. Liu, H. Shan, X. Chen and J. Gao, *Nano Lett.*, 2019, **19**, 5394-5402.
6. X. Liu, Y. Chen, H. Li, N. Huang, Q. Jin, K. Ren and J. Ji, *ACS Nano*, 2013, **7**, 6244-6257.